Comparison of Three Methods for Oscillating Flow Measurements in Cryocoolers

R. Snodgrass, V. Kotsubo, J. Ullom

National Institute of Standards and Technology, Boulder, CO
University of Colorado, Boulder, CO

ABSTRACT

Measurement of oscillating mass flows is typically required for the study of cryocoolers and cryocooler compressors. Although many measurement techniques are used in the cryocooler literature, detailed comparisons are lacking, so it can be challenging for experimentalists to decide which method(s) may be most appropriate for them. In this study, oscillating helium at flow rate magnitudes up to about 10 g/s were simultaneously measured using three different techniques: hot wire anemometry, measurement of the pressure difference across a bed of screens and measurement of the pressure oscillation in a reservoir of known compliance. It is shown that these three flow meters agree with one another to within a few percent of the maximum flow rate; this agreement validates all three methods as viable tools for the cryocooler experimentalist. The flow meter based on the compliance of a reservoir is most accurate when accounting for thermal boundary layer effects. Mass flow rates were measured near ambient temperature and at a frequency of 1.4 Hz.

INTRODUCTION

Mass flow rate measurements are fundamental to the experimental study of cryocoolers. They are required to determine the flow of important thermodynamic quantities including exergy, entropy, acoustic power, and others. A wide variety of flow measurement techniques are available [1], each with distinct advantages and disadvantages. Some have limitations in accuracy and response time, while others introduce disturbances to the experiment that may be unacceptable.

One way to probe volumetric flow rate is by measurement of the pressure oscillation in a reservoir of known compliance (for brevity we will refer to this as the compliance method). It is usually simple to take this measurement, since pressure transducers are common and easy to use and the compliance of the reservoir can be calculated from its geometry. Two major advantages of this technique are that no calibrating flow meter is needed and no construction may be required, since reservoirs are commonly used in cryocoolers (such as in the terminating networks of pulse tube refrigerators). Because of its simplicity, we previously utilized this technique for measurement of acoustic power flow [2]; however, we were disappointed that we could find no validation of it against other flow meters.

Two other common techniques are hot wire anemometry and measurement of the pressure difference across a bed of screens. These methods are more complicated to implement compared to the compliance method because they must be calibrated against another flow

Cryocoolers 23, edited by R.G. Ross, Jr. and J.R. Raab

meter. Calibration can be a significant effort, especially for users who have not previously acquired the equipment and expertise required. For example, an entirely new experiment may need to be built that connects the flow meters of interest to a source of gas that can deliver steady flow across a wide range of flow rates. Temperature control of the flow is also required if using hot wire anemometry.

The purpose of this study is twofold. First, we believe it is valuable to simultaneously measure identical flows with the three flow meters just described. If the three meters yield the same mass flow rate, then they validate one another and confirm that any would be appropriate for the cryocooler experimentalist (at least in flow conditions similar to those studied here). If the three meters disagree, then we can begin to study under what conditions the flow meters fail. The second purpose of the study is to give practical guidance to those considering different flow measurement techniques: highlighting advantages, disadvantages and methodology.

Description of the three flow measurement techniques

A hot wire anemometer is a flow rate meter composed of a very thin, relatively long wire that is held in a flow channel and regulated to a constant temperature. This temperature should be significantly greater than the temperature of the flow. For a properly constructed hot wire anemometer, the heat removed by the flow balances the heat required to electrically regulate the wire to a constant temperature. Typically, the wires are made of tungsten (because it is durable and has a fairly high temperature coefficient of resistivity [3]), are a few μm in diameter, and a few mm long. Such geometry ensures that the heat transfer by conduction to support structures is very small, and also results in rapid response times: usually just fractions of a millisecond. They are commonly used in turbulence studies.

The hot wire is electrically connected as one leg of a bridge circuit and the output of the bridge is amplified and fed back to the bridge input; the required electronics are commercially available or can be inexpensively built [4]. After calibration, the bridge voltage can be used to find the mass flow rate if the temperature of the flow is also measured, this is typically achieved by a second wire identical to the hot wire except driven with a small, constant current. This thermometer is often called the cold wire. More specifics on this method are available in multiple, excellent references [5,6].

Flow rate may also be found by measuring the pressure difference across a bed of randomly stacked screens. The pressure difference is a combination of viscous and inertial effects, and so depends on the Reynolds number. The Reynolds number of interest is defined by the hydraulic diameter D_h of the screen bed, which is

$$D_h = d_w\varphi/(1-\varphi) \tag{1}$$

In the above, d_w is the wire diameter and φ is the screen bed porosity, estimated with

$$\varphi \approx 1 - \pi n d_w/4 \tag{2}$$

where n is the number of holes in the screen per unit length. Finally, the Reynolds number Re_h is expressed in terms of the mass flow rate $\dot{m}$:

$$Re_h = \dot{m}D_h/\mu A\varphi \tag{3}$$

where μ is the dynamic viscosity and A is the area of the flow channel into which the screens are packed.

At sufficiently high Re_h (about 1000 or higher), viscous effects are relatively small, and the pressure difference across the screen bed Δp is proportional to the dynamic pressure $\rho u^2/2$, where ρ is the gas density and u is the flow velocity. In this regime $\dot{m}$ can be calculated by measuring the density of the gas in the screens and the pressure difference across them. At lower Re_h, accurate mass flow rate measurements can still be made, but viscous effects must be accounted for through

a Reynolds-number-dependent friction factor. There is much literature on this topic and friction factors are defined in many ways, but we take the approach outlined in [7]. In that work, the Fanning friction factor f_F (equal to the Darcy friction factor divided by four) is:

$$f_F = \rho \Delta p \left(\frac{A\varphi}{\dot{m}}\right)^2 \frac{D_h}{2L} \tag{4}$$

where L is the length of the screen bed, and we have converted flow velocity to mass flow rate. The above can be rearranged to see that

$$\dot{m} \propto \sqrt{\rho \Delta p / f_F} \tag{5}$$

where the proportionality constant is dependent upon the geometry of the screen bed and may be found through a calibration procedure (discussed later). The friction factor is also measured during calibration as a function of Re_h.

When using Eq. 5 to calculate mass flow rate, ρ and Δp will be measured by a variety of sensors in the experimental apparatus; however, the friction factor must be compared to calibration data that itself requires knowledge of the flow rate. Therefore, at low Re_h (where f_F cannot be approximated as a constant value) an iterative procedure is required to calculate $\dot{m}$.

Now we proceed by discussing the third and final flow measurement technique: measuring the pressure oscillation in a reservoir of known compliance. The compliance of a volume V undergoing adiabatic oscillations is $C = V/\gamma p$, where γ is the ratio of isobaric to isochoric specific heats, and p is the pressure [8]. The volumetric flow rate entering and exiting the volume is $U = Cdp/dt$.

The above analysis assumes that all of the gas in the volume undergoes adiabatic oscillations; however, thermal conduction between the gas and the wall decreases the magnitude of the temperature oscillation of the gas within the thermal boundary layer. In the thermoacoustic literature this effect is referred to as thermal relaxation. Thermal relaxation impacts the simplified version of the volumetric flow rate described in the previous paragraph because the portion of the gas that is in thermal contact with the wall requires more flow to be compressed. Starting with the thermoacoustic expression for U in a compliance [9] and converting to the time domain, the volumetric flow rate into a reservoir is approximately

$$U(t) \approx \frac{1}{\gamma p(t)} \left[(V + \alpha) \frac{dp(t)}{dt} + \omega \alpha \left[p(t) - \overline{p(t)} \right] \right] \tag{6}$$

Equation 6 can be converted to $\dot{m}$ by multiplying with the density of the gas entering/leaving the reservoir. In the above, t is time, ω is the angular frequency, p is the pressure in the reservoir, the overline represents cycle mean, and α is defined as

$$\alpha = S\delta_\kappa(\gamma - 1)/2(1 + \varepsilon_s) \tag{7}$$

where S is the interior surface area of the volume, δ_K is the thermal penetration depth and ε_S is defined in [9] but is usually very close to zero. Equation 6 shows that U (and $\dot{m}$) would be underestimated if thermal boundary layer effects were ignored. This equation is an approximation because it only converts the adiabatic portion of the compliance into the time domain; thermal boundary layer effects still rely on thermoacoustic definitions. However, as we show later, this approximation calculates flow rates that are in excellent agreement with the other two flow meters.

EXPERIMENTAL METHODS

Flow meter construction and equipment

Both the hot wire anemometer and the pressure difference flow meter were built into a single assembly inspired by a previous design [5]. The assembly is made from a commercially available gasket seal cross fitting, as shown in Fig. 1. Helium flows through one channel in the cross, while the perpendicular channel is occupied by replaceable fixtures that hold the hot and cold wires.

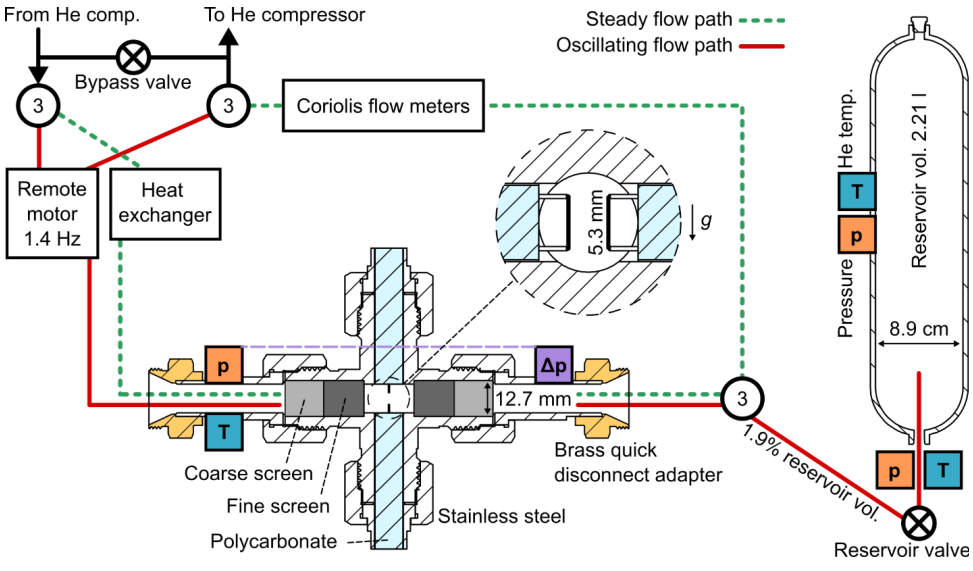

Figure 1. Experimental apparatus for the calibration procedure (dotted green line) and oscillating flow measurements (solid red line). In the flow assembly (bottom) the portion of the quick disconnect fittings which form seals is not displayed. The remote motor is the same type typically used in low-frequency pulse tube refrigerators. Diverting valves are shown by the number 3. Please see text for more details.

We proceed by describing the hot wire anemometer in more detail. Although it is currently possible to purchase hot wire probes directly from manufacturers, we decided that such probes were prohibitive in regard to their design and price. For example, the only affordable, off-the-shelf hot wire probes found were 5 µm in diameter, 1.25 mm long, and would not easily mount into the flow assembly. Instead of purchasing these probes, we built our own using longer, thicker wires and a simple cylindrical probe support made of polycarbonate. The polycarbonate (Fig. 1) electrically isolates the cross fitting from the tungsten wires and the rigid brass posts which the wires are soldered onto. To achieve pressure-tight seals, the polycarbonate cylinders were epoxied into off-the-shelf, stainless steel gasket seal fittings (as done in [5]).

Gold-plated tungsten wire was chosen for the anemometer because it is affordable, available in a large variety of diameters, and can be soldered to the brass support posts without any specialized equipment. Soldering was made easier with use of a stereo microscope and a custom fixture to hold the wires taught. After soldering, the flux was removed, and the wire ends were clipped by repeatedly twisting the wires. The result is displayed in Fig. 2. The wire in our custom probes is 15 µm in diameter and about 5.3 mm long, with a measured resistance of 1.48 ohms at 295 K. They can be lightly touched with a tweezer without damage and never showed signs of breaking while inside the flow assembly.

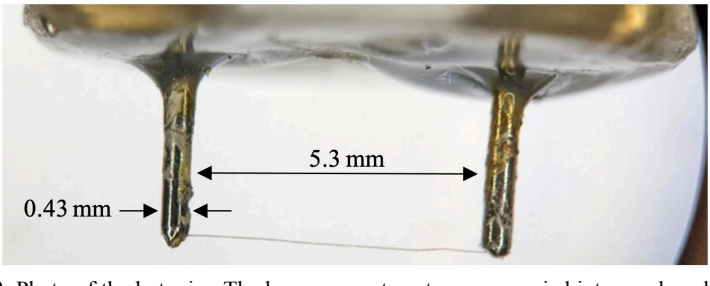

Figure 2. Photo of the hot wire. The brass support posts were epoxied into a polycarbonate cylinder. The cold wire (not shown) is similar.

The hot wire was regulated to 2.96 ohms (twice its resistance at 295 K) using a TSI IFA300. The IFA300 can apply a lowpass filter in hardware, but this resulted in a phase lag; instead the hot wire signal was filtered in software. The cold wire is identical in construction to the hot wire but, instead of being regulated to a constant temperature (resistance), was driven with a constant current (8.37 mA, which resulted in 0.1 K of self heating in stagnant 1.3 MPa helium). When a square wave impulse was applied to the cold wire in stagnant helium it took about 6 ms for its temperature (resistance) to reach a steady value; its response in actual flow conditions should be much more rapid but is not easily measured.

A series of screens was installed in the flow assembly for two purposes. As recommended in [5], screens act as flow straighteners and help to achieve flow uniformity across the hot and cold wires. The second purpose of the screens is to generate a pressure drop for the other flow meter. As shown in Fig. 1, screens were placed on both sides of the hot and cold wires, and two different screen sizes were used. A stack of 35 stainless steel screens of mesh size 60 (n = 2.36 holes/mm, d_W = 0.191 mm) were placed nearest the hot and cold wires, adjacent to 20 stainless steel screens of mesh size 20 (n = 0.787 holes/mm, d_W = 0.406 mm). Since this stack was placed on both sides of the assembly the total number was 70 fine screens and 40 coarse screens.

Two piezoresistive pressure transducers were placed in the flow channel: one to measure the absolute pressure (Endevco 8510B-500) and the other to measure the pressure difference across the two screen beds (Endevco 8510C-100). The response time of these transducers is about 5 μs. The absolute pressure at the location of the hot and cold wires was assumed to be the average of the absolute pressures on the ends of the assembly and together with the cold wire measurement was used to determine the gas density near the wires. This is the density that was used for the pressure difference flow meter, although it only serves as an estimate for the true density at any location in the screen beds. A commercial RTD (resistance temperature detector) in a stainless steel sleeve was also installed in the assembly near the absolute pressure transducer and was used to calibrate the cold wire. To ensure that these two sensors were at the same temperature during calibration, high helium flow rates were used, and the portion of the probe containing the RTD was completely submerged into the flow.

We estimate that the plumbing between the flow assembly and the reservoir occupies a volume equal to about 1.9% of the reservoir volume. Therefore V (Eq. 6) was taken as 1.019 times the measured reservoir volume (found by weighing the water required to fill it). To measure gas density, pressure and temperature were recorded at two different locations in the reservoir: at its inlet and near its center. Temperature at the inlet was measured by a 36 AWG, T-type thermocouple with cold junction compensation, while temperature in the reservoir was measured by a cold wire similar to that in the flow assembly except with longer supports, so that the tungsten wire was at least 1 cm from the interior wall of the reservoir. We made sure not to place pressure transducers opposite the inlet of the reservoir because of flow stagnation [10]. A globe valve was installed near the inlet of the reservoir, but (unless otherwise stated) was kept completely open.

The two ends of the flow assembly were connected to quick disconnect fittings using 94/6 tin/silver solder. This enabled the flow assembly to be disconnected and modified without depressurizing other parts of the experiment.

Calibration methodology

The completed flow assembly was placed into a fluid circuit (dashed green line in Fig. 1) driven by a Cryomech CP2850 helium compressor. This compressor is an oil-lubricated scroll, consumes about 7 kW of electricity and is typically used to provide flow to low-frequency, 4 K pulse tube refrigerators. A bypass valve was placed between the high and low sides of the compressor to vary the mass flow sent to the flow assembly. The fluid circuit was filled with ultra-high purity helium to a pressure near 1.4 MPa.

Mass flow was measured using two different Coriolis flow meters, both manufactured by Endress+Hauser. The larger of the two flow meters (Promass 83F08) can measure flows between about 0.6 g/s and 21 g/s to an accuracy near ± 0.35% of reading. The smaller Coriolis flow meter (Promass 83A02) can measure flows up to about 2 g/s with an accuracy close to ± 0.5% of reading.

For calibration flow rates less than about 1 g/s the flow was sent through both meters, but the measurement from the smaller flow meter was used, while for higher flow rates the smaller Coriolis was bypassed (valves not shown in Fig. 1). When flow was simultaneously sent through both meters they agreed to within repeatability limits, validating their factory calibrations. Besides being extremely accurate, Coriolis flow meters also benefit from gas-independent calibration; however, their relatively slow response time limits their use to steady flow conditions.

To control the temperature of the flow leaving the compressor, a heat exchanger was installed between it and the flow assembly. This heat exchanger was heated by an array of resistive heaters and cooled by a pulse tube refrigerator connected to another CP2850 helium compressor.

Each calibration point was collected as follows. After the heat exchanger was heated the compressor was turned on. Shortly after turning on the compressor the pulse tube refrigerator was started to cool the heat exchanger. We collected calibration data at fixed mass flow rates at temperatures between about 298 and 292 K. The mass flow rate was typically constant (within repeatability limits of the Coriolis) but sometimes drifted slightly over time. This process was repeated at different flow rates by changing the flow impedance of the bypass valve.

The entire calibration procedure was completed with the flow assembly installed in the forward flow direction (mounted in the same orientation as when oscillating flow measurements were made) and in the reverse direction (flipped 180°).

Oscillating flow methodology

The fluid circuit that the flow assembly was installed into was designed such that a series of three-way diverting valves (labeled "3" in Fig. 1) could be turned to switch between the calibration procedure and oscillating flow measurements. Besides being very convenient, this ensured that it was not possible to unintentionally disturb the sensors after calibration, as might have occurred if it was necessary to remove the flow assembly and install it in a different apparatus.

The same bypass valve used to vary the flow rate during calibration was used to vary the magnitude of the oscillating flow. When the bypass valve was completely closed and the system was driven at 1.4 Hz, the pressure amplitude normalized by the mean pressure (p_1/p_m) was about 0.35. The amplitude was measured as (p_h - p_l)/2 and the mean as (p_h + p_l)/2, where p_h and p_l are the high and low pressures (respectively) in the reservoir. All signals required to calculate mass flow rates were sampled simultaneously at 976 Hz using a Labjack T8. At least six full, sequential oscillations were collected for each bypass valve setting.

RESULTS

Now we present the results of the calibration and oscillating flow measurements. For succinctness we refer to the mass flows measured by the hot wire anemometer, the pressure difference flow meter, and the compliance method as $\dot{m}_h$, $\dot{m}_p$, and $\dot{m}_c$, respectively.

Calibration results

Figure 3 shows the calibration data for the pressure difference flow meter. The Fanning friction factor was measured for mass flows between 0.13 and 6.8 g/s (the highest the compressor could deliver). In the literature it is common to fit the data to a function $f_F = aRe_h^{-1} + b$. Our result is $f_F = 30.1Re_h^{-1} + 0.175$, which is reasonably close to the $f_F = 32Re_h^{-1} + 0.3$ from [7]; however, our results are not directly comparable because our experiment used two screen sizes instead of one. When calculating f_F we made the crude approximation that the entire screen bed was composed of the finer screen. Because it provides a better fit, we always used a cubic spline fit to the f_F data (Fig. 3a) when calculating $\dot{m}_p$.

Figure 3b plots $\dot{m}_p$ (measured with the Coriolis meters) against $\sqrt{\rho\Delta p/f_F}$ for both the forward and reverse flow directions. A linear fit to these data produces a Pearson correlation coefficient of 0.99995. Since the forward and reverse flow directions produced very similar fits (slopes matching to better than 2%) we only used one fit (from the forward direction) when calculating $\dot{m}_p$. The pressure transducer manufacturer guarantees that the forward and reverse sensitivities match to within 1%.

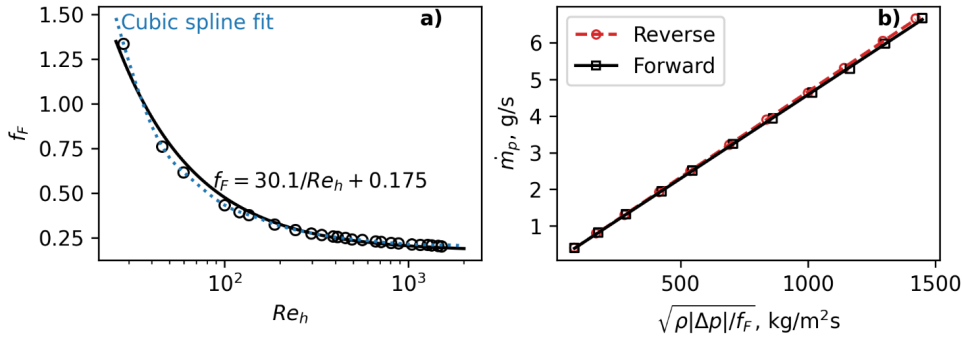

Figure 3. Calibration data for the pressure difference flow meter. Please see text for more details.

The calibration data for the hot wire anemometer is shown in Fig. 4. The first panel plots the bridge voltage E squared between 292 K and 298 K for many different flow rates (only the data for the reverse direction is shown). The slopes of those lines at 295 K are plotted in Fig 4b; although we do not discuss the details here, these slopes are used to scale the bridge voltage when the cold wire is at temperatures not equal to 295 K (see [5]). Figure 4c shows power law fits of $\dot{m}_h$ (measured with the Coriolis flow meters) against E^2 at 295 K for both flow directions. The two flow directions produced significantly different calibrations, so (when calculating $\dot{m}_h$ during the subsequent oscillating flow measurements) we were forced to interpret the direction of flow and choose the correct calibration curve. The direction dependence of the hot wire anemometer is a significant disadvantage for this flow technique. We do not believe it is a fundamental limitation, rather we suspect it is an artifact of our construction methodology. Because the hot wires were made by hand, we were unable to mount the wires at the extreme end of the support posts (Fig. 2).

Some evidence of hysteresis (not shown) was observed during calibration of the hot wire anemometer. When flow first started the temperature of the helium would quickly rise due to the heat exchanger being hot and would slowly cool over time. In some instances, we observed slightly different bridge voltages for the same cold wire temperature and the same mass flow rate, depending on whether the flow was increasing or decreasing in temperature. This may suggest that the hot and/or cold wires were affected by the temperature of the flow assembly. It's possible that this issue may have been avoided by mounting the wires on longer supports.

Oscillating flow results

Oscillating flow was measured at 11 different pressure amplitudes. An example of the important sensor data is presented in Fig. 5 for a single pressure amplitude. The calculated mass flow rate is plotted in the top row of Fig. 6 for three pressure amplitudes. Visual inspection of the

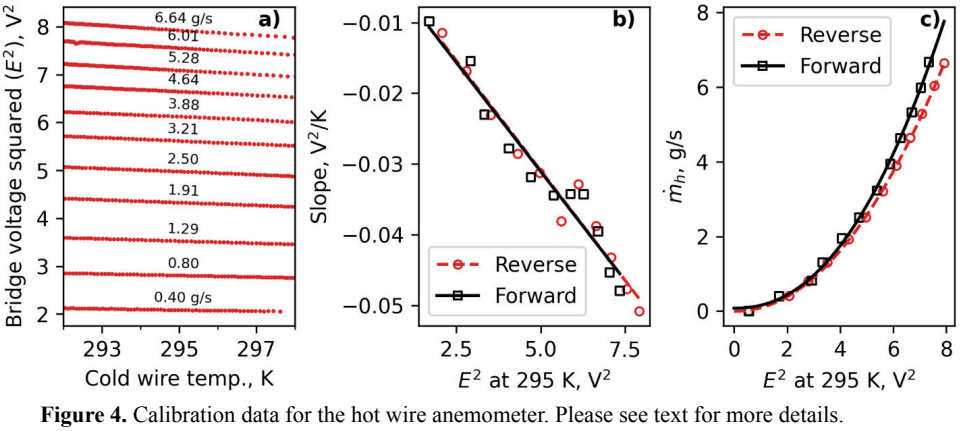

Figure 4. Calibration data for the hot wire anemometer. Please see text for more details.

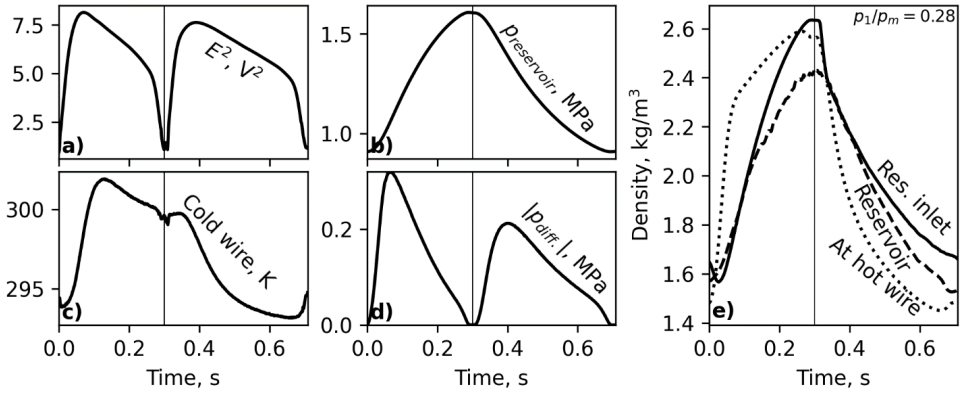

Figure 5. Example sensor data for a single cycle. E is the bridge voltage for the hot wire. Vertical line shows approximately when the flow changes direction (as determined by the minimum of E).

top row shows that the three methods yield nearly the same $\dot{m}$. The difference between methods (usually a few tenths of a g/s) is plotted in the bottom row. The brown line in the bottom row of Fig. 6 also plots the difference between the pressure difference meter and the compliance method when boundary layer effects were neglected: this line is labeled as $\dot{m}_{c,nobl}$ and was calculated with Eq. 6 but with $\alpha = 0$. Comparison of the brown and orange lines show that the agreement is significantly worse when neglecting thermal relaxation.

The quantitative agreement between the three methods can be summarized by measuring the time-average difference between the signals. Figure 7a shows that the hot wire anemometer and pressure difference meter typically agree to within 2% of the maximum flow rate, while the compliance method and the pressure difference meter typically agree to within 1.5% of the maximum flow rate (this difference

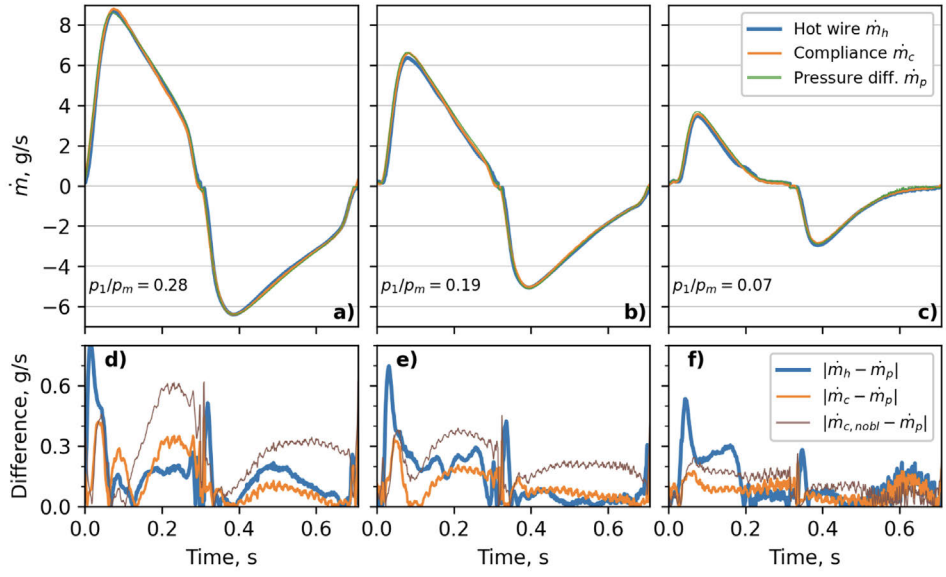

Figure 6. (Top) Oscillating flow of helium at a mean pressure near 1.4 MPa and a temperature near 295 K. Positive values correspond to mass entering the reservoir. (Bottom) The absolute difference in the mass flow rates as calculated by the three meters; $\dot{m}_{c,nobl}$ is calculated by the compliance method when ignoring boundary layer effects. Each column plots a different pressure amplitude.

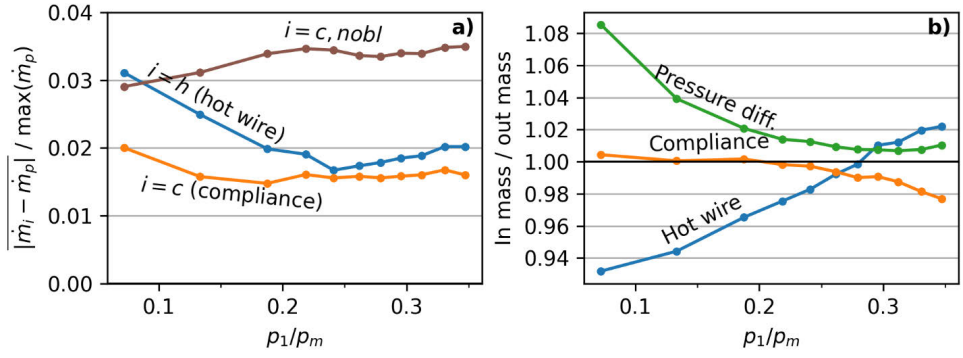

Figure 7. a) The average difference in $\dot{m}$ normalized by the max of $\dot{m}$ (as a function of pressure amplitude). The brown line labeled "*i=c,nobl*" is the difference between the pressure difference meter and the compliance method when calculated ignoring boundary layer effects. b) Over at least six full oscillations, the total mass entering the reservoir normalized by the total mass leaving the reservoir.

jumps to around 3.5% if boundary layer effects are neglected). Average agreement changes at low pressure amplitudes because of the poor sensitivity of the Δp measurement at low flow rates ($\Delta p \propto u^2$).

It is possible to independently quantify the accuracy of the methods by comparing the total mass that flows into the reservoir with the total mass that flows out of the reservoir. Over an integer number of cycles, these should be equal since no mass accumulates in the reservoir. As shown in Fig. 7b, the pressure difference meter gives excellent agreement between the in and out masses except at low pressure amplitudes. This is explained by the poor sensitivity at low flow rates: for example, at a flow rate of 0.2 g/s the pressure transducer was operating at a Δp of only about 0.1% of full scale. The compliance method has excellent agreement for the in/out masses except at the highest pressure amplitudes. Although we haven't studied this result in detail, it may be explained by greater variations in gas density at the inlet of the reservoir (we only estimated density with a single thermocouple and pressure transducer at that location). Of the three flow methods, the hot wire anemometer has the worst agreement for total in and out mass. That the curve trends clearly in one direction may suggest that the hysteretic effects discussed earlier are responsible (the 11 pressure amplitudes were collected sequentially starting at the highest and ending with the smallest).

In another set of experiments (not shown) we almost completely closed the valve between the flow assembly and the reservoir, creating a large flow impedance. Under these conditions, the flows calculated by the hot wire and the pressure difference measurement were sometimes significantly higher than those calculated by the compliance measurement (this was especially true when mass began to move into the reservoir). We hypothesize that this discrepancy occurs because a significant amount of mass is required to increase the pressure (and density) of the gas between the flow assembly and reservoir valve. This observation suggests that gradients in gas density must be considered when significant flow impedances are present in the flow network.

CONCLUSION

It is encouraging that these three flow methods typically agree with one another to within a few percent of the maximum flow rate. This study was operated at high pressure amplitudes and a relatively low frequency; however, these methods should also be appropriate for measurement of flows at significantly higher frequencies, since all required sensors have rapid response times. Boundary layer effects should be considered when measuring flow using the compliance method, although these effects should be less important at higher frequencies. We summarize the requirements and disadvantages of each flow measurement technique in Table 1.

Table 1. Summary of the three flow meters.

Technique	Required measurements	Disadvantages
Hot wire anemometry	○ Bridge voltage ○ Cold wire voltage	○ Requires calibration ○ We observed hysteresis and direction dependence ○ Construction may be challenging ○ Electronics may be expensive ○ Is it acceptable to heat the flow?
Pressure difference across screen bed	○ Pressure difference ○ Absolute pressure (for ρ) ○ Temperature (for ρ)	○ Requires calibration ○ Poor sensitivity at low flow rates ($\Delta p \propto u^2$) ○ Is it acceptable to introduce Δp into the flow?
Pressure oscillation in a reservoir of known compliance	○ Geometry of reservoir ○ Absolute pressure ○ Temperature (for ρ)	○ Terminating measurements only ○ For the best accuracy, boundary layer effects must be accounted for

ACKNOWLEDGMENTS

We would like to thank Ray Radebaugh and Gregory Swift for many helpful discussions on this topic. We acknowledge support from the Professional Research Experience Program between the University of Colorado Boulder and NIST (award number 70NANB18H006). Contribution of NIST, not subject to copyright. Certain equipment, instruments, or materials are identified in this paper in order to specify the experimental procedure adequately. Such identification is not intended to imply recommendation or endorsement by NIST, nor is it intended to imply that the materials or equipment identified are necessarily the best available for the purpose.

REFERENCES

1. R. Radebaugh, "Cryogenic Measurements, in Handbook of Measurement in Science and Engineering," *John Wiley & Sons, Ltd*, (2016), pp. 2181–2224.
2. R. Snodgrass, V. Kotsubo, S. Backhaus, J. Ullom, "Dynamic Acoustic Optimization of Pulse Tube Refrigerators for Rapid Cooldown," *Nat. Commun.,* 15, 3386, (2024).
3. W. Rawlins, R. Radebaugh, K. D. Timmerhaus, "Monitoring Rapidly Changing Temperatures of the Oscillating Working Fluid in a Regenerative Refrigerator, in Applications of Cryogenic Technology," *Springer US*, Boston, MA, (1991), pp. 71–83.
4. D. M. Birch, J. F. Morrison, "An Innovative Low-Profile Monolithic Constant-Temperature Anemometer," *J. Wind Eng. Ind. Aerodyn.,* 100, 38, (2012).
5. W. Rawlins, R. Radebaugh, K. D. Timmerhaus, "Thermal Anemometry for Mass Flow Measurement in Oscillating Cryogenic Gas Flows," *Rev. Sci. Instrum.,* 64, 3229, (1993).
6. H. H. Bruun, "Hot-Wire Anemometry: Principles and Signal Analysis," *Oxford University Press,* (1995).
7. R. S. Wakeland, R. M. Keolian, "Measurements of Resistance of Individual Square-Mesh Screens to Oscillating Flow at Low and Intermediate Reynolds Numbers," *J. Fluids Eng*., 125, 851, (2003).
8. G. W. Swift, "Thermoacoustics: A Unifying Perspective for Some Engines and Refrigerators," 2nd ed., *Springer International Publishing*, (2017).
9. B. Ward, J. Clark, G. Swift, *Users Guide for DeltaEC: Design Environment for Low-Amplitude Thermoacoustic Energy Conversion*, www.lanl.gov/thermoacoustics.
10. G. W. Swift, P. S. Spoor, "Jet-Induced Phase Errors in Pulse Tube Refrigerator Compliance Pressure," Cryocoolers, 20, (2018).